Fisher-Tropsch Synthesis on Alumina Supported Iron-Nickel Catalysts: Effect of Preparation Methods

M. Sarkari,[a,*] F. Fazlollahi,[b] A. Razmjooie,[c] and A. A. Mirzaei[d]
[a]Young Researchers Club, Shiraz Branch, Islamic Azad University, Shiraz, Iran
[b]Department of Chemical Engineering, Faculty of Engineering,
University of Sistan & Baluchestan, P.O. Box 98164-161, Zahedan, Iran
[c]South Zagros Oil and Gas Production Company, Dalan, Iran
[d]Department of Chemistry, Faculty of Science,
University of Sistan & Baluchestan, P.O. Box 98135-674, Zahedan, Iran

Original scientific paper
Received: April 21, 2011
Accepted: August 29, 2011

Two 40 % Fe/60 % Ni/Al_2O_3 catalysts were prepared using incipient wetness (catalyst A) and co-precipitation (catalyst B), and the activity and selectivity to light olefins in Fischer-Tropsch Synthesis (FTS) has been studied in a fixed-bed reactor under different operating conditions. These conditions were: temperature 220–270 °C, Pressure 1–15 bar, H_2/CO molar ratio 1–3 and gas hourly space velocity (GHSV) 1600–5600 h^{-1}. The optimum operating conditions were found for each catalyst and were used to study catalytic performance after stabilization. The results showed that these catalysts were highly stable and retained activity and selectivity for 240 h. The results also showed that the incipient wetness catalyst had a higher activity, higher selectivity to light olefin and C_{5+} products and lower selectivity to methane and water-gas shift (WGS) activity after stabilization. Also, it was found that higher iron dispersion enhances the negative effects of water such as low CO conversion, low olefin selectivity and higher methane and CO_2 selectivity.

Key words:
Fischer-Tropsch synthesis, iron nickel, co-precipitation, incipient wetness, light olefin

Introduction

In recent years, fast depletion of liquid fossil fuel reserves, the uncertainty in the Middle East and environmental pollution have driven a major shift in the focus of research in the energy production area. The FTS is at the heart of the gas to liquid (GTL) process that is one of the main methods of utilizing natural gas, as an alternative to the use of limited crude oil resources.[1–3] Depending on the catalysts employed, the main products are olefin, paraffin and oxygenate.[4]

Among the candidate transient metals only Co and Fe based catalysts have been developed for industrial use due to their cost, activity and selectivity.[5,6] The other metals active in the synthesis, namely nickel and ruthenium, were usually used only as promoters of cobalt and iron-based catalysts.[3] In order to develop catalysts that increase selectivity, additional information is required regarding FT reactions, whereas catalyst composition exerts the greatest influence on the molecular weight distribution (MWD) for the FTS products. Mixed metal catalysts are often capable of activity, selectivity, or have a stability, that is unobtainable with a single component[7] and it is believed that bimetallic catalysts system, due to the thermodynamic and kinetic limitations of the reaction, are more able to raise the value of the light olefins.[8–11]

Mixtures of iron and nickel oxides are effective catalysts for conversion of synthesis gas to desired products.[12] Nickel is well known as a methanation catalyst,[13] giving rise to an alkene/alkane ratio less than one in carbon monoxide hydrogenation, while it is generally accepted that the primary products of FTS reaction over iron catalysts are α-olefins and other properties are higher conversion, selectivity to lower olefins, and flexibility to process parameters.[14–17] It seems that the protection of the spinel phase under the reaction conditions and the presence of a metallic phase, which does not carburize under test, are essential to produce C_2–C_4 olefins from CO/H_2.[6,8,18,19]

In this study, two types of iron-nickel catalysts were prepared using incipient wetness and co-precipitation and the effect of inlet H_2/CO ratios, temperature, pressure and GHSV on the activity and selectivity to light olefinic product has been studied in a fixed-bed reactor. Optimum conditions were established for each catalyst and employed to test catalytic performance.

*Corresponding author. Tel.: +98 9368512260.
E-mail address: sarkari.majid@gmail.com (M. Sarkari)

Experimental

Catalyst preparation

In this study incipient wetness and co-precipitation were employed. In incipient wetness Al_2O_3 (surface area, 162.0 $m^2\ g^{-1}$; pore volume, 0.42 $cm^3\ g^{-1}$) was heated at 400 °C for 6 h. Then Al_2O_3 was impregnated with mixed aqueous solutions of $Ni(NO_3)_2 \cdot 6H_2O$ and $Fe(NO_3)_3 \cdot 9H_2O$ (both of 99.9 %, Merck, 0.25 mol L^{-1}) containing 40 % Fe and 60 % Ni. The catalysts were dried at 120 °C for 12 h after each impregnation step and then calcined at 600 °C for 6 h.

In the co-precipitation, aqueous solutions of $Fe(NO_3)_3 \cdot 9H_2O$ (5.89 g) and $Ni(NO_3)_2 \cdot 6H_2O$ (6.07 g) were pre-mixed, and the resulting solution was heated to 70 °C in a reflux flask equipped with a condenser. Aqueous Na_2CO_3 (99.8 %, Merck, 0.25 mol L^{-1}) was added dropwise to the mixed nitrate solution with stirring, while the temperature was maintained at 70 °C until pH = 8±0.1 was achieved. The 180 min aged precipitate was then filtered and washed several times with warm distilled water until no further Na^+ was observed in the filtrate (tested by flame atomic absorption). The precipitate was dried at 120 °C for 16 h and subsequently calcined at 600 °C for 6 h to give the final catalyst. Then, for the preparation of Al_2O_3 supported catalyst, the optimal amount of w = 40 % of γ-Al_2O_3 based on the total catalyst mass was added to the mixed solution of iron and nickel nitrates with the molar ratio of 40 % Fe/60 % Ni and then filtered, washed, dried at 120 °C and calcined at 600 °C for 6 h, in the same way as the unsupported catalyst preparation. All catalysts were sieved to a particle size < 150 μm to avoid internal mass transport limitations.[20]

The surface area and pore characteristics were measured employing a NOVA 2000 instrument (Quan-tachrome, USA) and X-ray diffraction was performed using a Siemens D5000 X-ray diffractometer with monochromatic Cu-Kα radiation. The morphology of catalysts and their precursors was observed by means of an S-360 Oxford Eng scanning electron microscope.

Analysis system

The FTS experiments were performed in a stainless steel fixed-bed micro-reactor with an inner diameter of 12 mm. The detailed description of reactor setup as well as a schematic diagram and analysis method can be found elsewhere.[8–11,19]

To summarize, three mass flow controllers equipped with a four-channel control panel were used to adjust automatically the flow rate of the inlet gases (CO, H_2, and N_2 with purity of 99.999 %). The mixed gases in the mixing chamber passed into the reactor tube, which was placed inside a tubular furnace capable of producing temperatures up to 1300 °C and controlled by a digital programmable controller (DPC). The reaction temperature was controlled by a thermocouple inserted into catalyst bed and monitored by a computer. The reactor was equipped with an electronic back pressure regulator with the ability of controlling total pressure between 1 and 100 bar. The two catalysts (A) and (B) was pre-reduced in situ at atmospheric pressure in a flowing H_2–N_2 stream (N_2/H_2 = 1, flow rate of each gas = 30 mL min^{-1}) at 400 °C for 10 and 6 h, respectively.

A portion of the unconverted reactants and the reaction products was sent to a gas chromatograph (GC) for on-line analysis after passing a knockout pot at ambient temperature and then into a vent line. The gas chromatograph was equipped with a 10-port sampling valve, flame ionization detector (FID) and thermal conductivity detector (TCD) and a capillary column. In this study the effects of operating conditions were examined by varying reaction temperature (230–270 °C), pressure (1–15 bar), gas hourly space velocity (1600–5400 h^{-1}) and H_2/CO feed molar ratio (1–3). The results in terms of CO conversion, selectivity and yield of products were given at each space velocity. The CO conversion (%) was calculated according to the standard method:

$$CO\ conversion\ (\%) = \frac{N_{CO,in} - N_{CO,out}}{N_{CO,in}} \cdot 100 \quad (1)$$

The selectivity (%) towards the individual components on carbon basis is calculated according to the same principle:

$$Selectivity_{(i)}(\%) = \frac{n_i N_i}{N_{CO,in} - N_{CO,out}} \cdot 100 \quad (2)$$

Carbon balance was calculated as follow:

$$Carbon\ balance\ (\%) = \frac{N_{C,out}}{N_{C,in}} \cdot 100 \quad (3)$$

Where, N denotes the number of moles, n is the atom carbon number, and i is the product i^{th}.

Result and discussion

Catalyst characterization

The optimal catalysts for the production of higher light olefins and low production of methane were 40 % Fe/60 % Ni/40% Al_2O_3. As illustrated in Fig. 1, for the impregnation catalyst (A) the phases

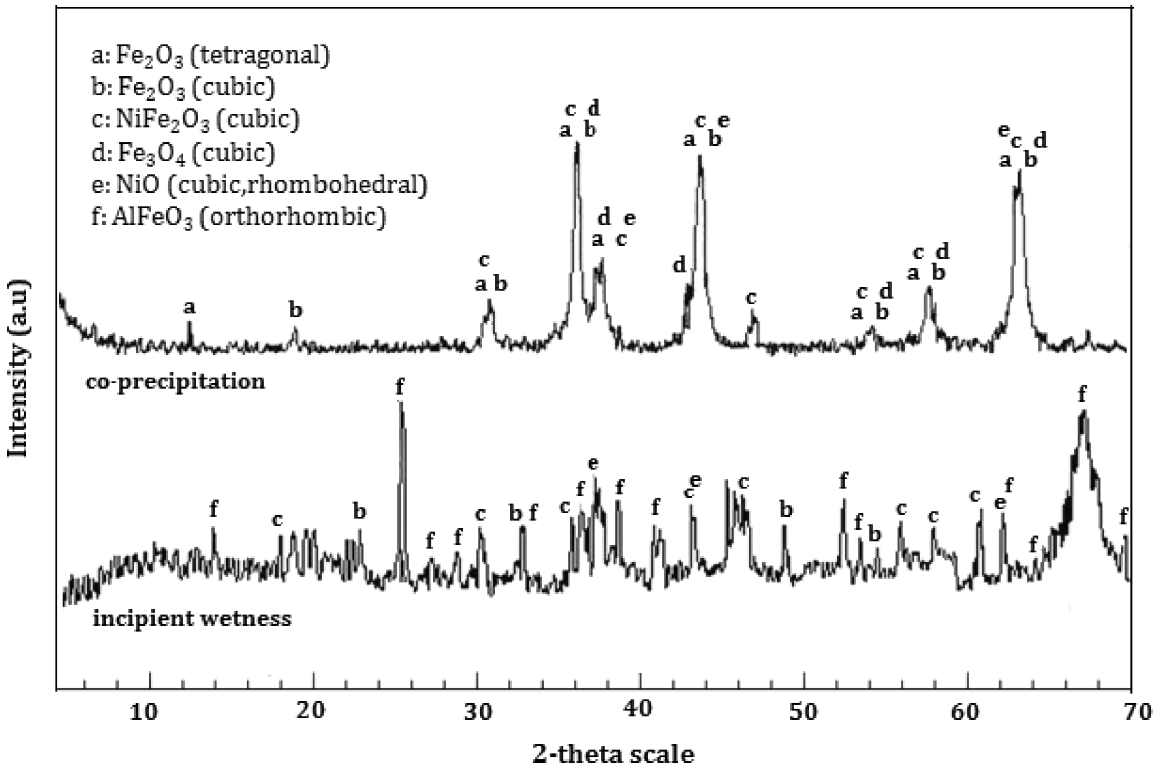

Fig. 1 – *XRD patterns for the calcined (fresh) catalysts containing 40 % Fe/60 % Ni/Al_2O_3, bottom: wetness catalyst (A) and top: precipitation catalyst (B)*

identified with XRD of the fresh catalyst (after calcination and before activation and testing) were NiO (cubic), $AlFeO_3$ (orthorhombic); Fe_2O_3 (cubic) and $NiFe_2O_4$ (cubic). For the co-precipitated catalyst (B), the phases were NiO (cubic and rhombohedral), $NiFe_2O_4$ (cubic), Fe_2O_3 (cubic) and Fe_3O_4 (cubic).

The used catalysts contain carbide (FeC, FeC_2, Fe_2C) and iron oxide (Fe_2O_3, Fe_3O_4) phases, both of which are active phases in FTS. Carbide phases have been reported to be active in the hydrogenation of CO, and oxide phases are highly selective for the production of olefins. Magnetite (Fe_3O_4) is the most active phase for the water gas shift reaction.[16,21–24]

The BET surface areas for the two catalysts are given in Table 1. The results show that, before the test, the calcined catalyst has a higher specific surface area than its precursor; this is in agreement with the results which showed that the agglomerate size of calcined catalyst is less than its precursor, and therefore leads to an increase in the BET specific surface area of the calcined sample. On the other hand, the used catalysts have a larger agglomeration size and lower specific surface area which may be due to sintering after FT reaction. These trends are the same for both catalysts. The highlight result is that the specific surface area of incipient wetness is larger than co-precipitation catalyst in each step.

Table 1 – *BET characterization of catalyst 40 % Fe/60 % Ni/40 % Al_2O_3*

Preparation method	Specific surface area (m^2 g^{-1})		
	Precursor	Calcined catalyst (fresh)	Calcined catalyst (used)
incipient wetness	121.0	154.5	152.3
co-precipitation	108.2	124.1	117.2

The SEM images of each catalyst are shown in Fig. 2. The SEM observations exhibit differences in morphology of precursor and calcined catalysts (fresh and used). The electron micrograph obtained from precursor show several larger agglomerations of particles (Fig. 2, top) and shows that this material has a less dense and homogeneous morphology. After the calcinations at 600 °C for 6 h for each catalysts, the morphological features are different with the precursor sample and show that the agglomerate size is greatly reduced compared to the precursor (Fig. 2, middle). This may be due to the fact that the calcined catalyst surface is covered with small crystallites of iron and nickel oxide, in agreement with XRD results. However, the size of these grains grew larger by agglomeration in the tested catalyst (Fig. 2, bottom), which may be due to the sintering after reactions and catalyst reduction.

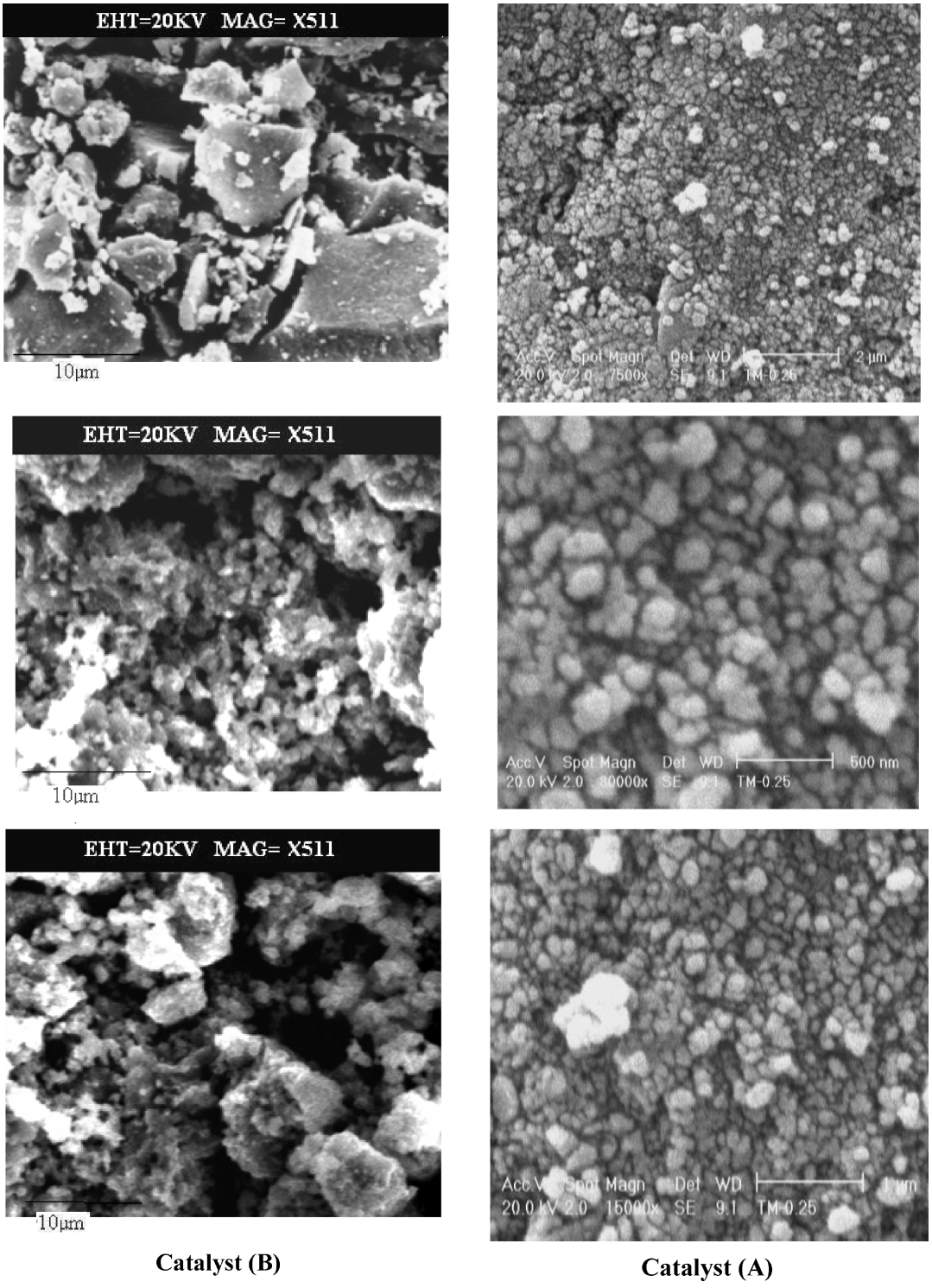

Fig. 2 – *The SEM images of catalysts containing 40 % Fe/60 % Ni/40 % Al_2O_3. (top) precursor, (middle) fresh calcined catalyst, (bottom) used calcined catalyst.*

Effect of process conditions

In this study, the effects of operating conditions were examined by varying reaction temperature (230–270 °C), pressure (1–15 bar), gas hourly space velocity (1600–5400 h^{-1}), and H_2/CO feed molar ratio (1–3).

Effect of H_2/CO molar feed ratio

The influence of syngas composition on FTS is shown in Table 2 for varying the H_2/CO inlet molar ratio (1, 1.5, 2, and 3) while keeping constant the other conditions at ϑ = 240 °C, p = 1 bar, GHSV = 3600 h^{-1}).

Table 2 – *Effect of H_2/CO molar ratio*

	Catalyst	H_2/CO (molar ratio)			
		1	1.5	2	3
CO conv. (%)	A	31.2	33.2	35.3	30.2
	B	45.6	50.3	58.9	53.1
Methane sel. (%)	A	21.4	24.1	20.8	25.1
	B	27.9	26.2	24.1	28.5
Olefin (C_2-C_4) sel. (%)	A	29.7	24.7	33.9	26.0
	B	28.6	27.8	32.2	23.1
C_{5+} sel. (%)	A	23.9	21.6	19.1	17.6
	B	13.3	11.7	11.4	9.9
CO_2 sel. (%)	A	6.8	7.4	6.3	7.5
	B	8.9	8.4	7.2	11.7

Table 3 – *Effect of temperature on CO conversion and selectivity*

	Catalyst	Temperature (°C)					
		220	230	240	250	260	270
CO conv. (%)	A	27.9	29.3	35.3	59.1	63.7	67.5
	B	41.7	49.5	58.6	59.0	61.0	65.8
Methane sel. (%)	A	18.5	20.1	20.8	21.2	21.4	22.7
	B	16.8	17.5	18.4	20.4	23.0	27.6
Olefin (C_2-C_4) sel. (%)	A	25.4	26.6	33.9	34.8	38.1	30.1
	B	31.2	33.8	37.2	36.0	33.8	29.8
C_{5+} sel. (%)	A	23.4	24.6	17.6	15.7	12.2	13.1
	B	14.5	14.7	13.9	12.8	12.8	10.9
CO_2 sel. (%)	A	5.1	5.9	6.3	6.5	6.4	7.5
	B	5.6	5.1	5.1	5.7	6.4	7.2

It is well known that H and CO coverage play essential roles in the reactivity and selectivity of FT synthesis. The results indicated that CO conversion increases with the increase of the H_2/CO molar feed ratio from 1/1 to 2/1, and after passing a maximum apex in H_2/CO = 2, activity decreases. It can be concluded that a low H_2/CO ratio leads to increased CO adsorption relative to hydrogen because it is well known that CO adsorption is stronger than the H on iron catalyst.[25] Therefore, the scarcity of surface H causes low activity. As H_2/CO ratio is increased to 3.0, the lower CO partial pressure induces a lower concentration of adsorbed CO, so that more H_2 can be adsorbed and dissociated. The lack of CO leads to a decrease in activity and less heavy hydrocarbons. This trend for the two catalyst types is the same. Methane selectivity also increases with H_2/CO. On the contrary, the selectivity to C_{5+} hydrocarbon decreases linearly upon increasing the H_2 content of feed gas. Selectivity toward the light olefin for both catalysts (A and B) is the highest value in H_2/CO = 2. As shown in Table 2, it can be concluded that water gas shift activity with respect to lowest CO_2 value shows the lowest activity for this molar ratio.

Comparison of the two catalysts' performance shows that the co-precipitation catalyst has higher activity, higher selectivity to CH_4 and higher WGS activity, and lower selectivity to light olefin and C_{5+} hydrocarbon. Thus, H_2/CO = 2 was chosen as the optimum ratio for conversion of synthesis gas to C_2–C_4 olefins over the iron nickel catalysts.

Effect of reaction temperature

The influence of reaction temperature was studied for 220–270 °C using the same reaction conditions (p = 1 bar, H_2/CO = 2/1 and GHSV = 3600 h^{-1}), and the results are presented in Table 3.

CO conversion strongly increases with temperature for both catalysts. Selectivity to methane also increases with temperature, but it has a stronger effect on catalyst (B). Selectivity toward light olefin for catalyst (A) increases until 260 °C and then decreases with temperature, while for catalyst (A) the maximum selectivity occurs at 240 °C. Temperature has a modest effect on chain growth probability (C_{5+} selectivity) for catalyst (B) while there was a significant effect for catalyst (A).

It is clear that for catalyst (A) at reaction temperature of 260 °C, the total selectivity of light olefin products was higher than the total selectivity of these products obtained at other reaction temperatures.

Effect of pressure

The effect of pressure on the FTS was studied at different pressure levels (1 to 15 bar), under the reaction conditions of H_2/CO = 2/1 and 260 °C (Table 4).

As shown in Table 4, for catalyst (A) the increase of total pressure slightly decreases the CO conversion from 64.1 % at 1 bar to 60 % at 15 bar. For catalyst (B), the CO conversion decreases from 58.6 to 51.3 %. In contrast, the selectivity to heavier hydrocarbons (C_{5+}) strongly increases with pressure, while the selectivity to both methane and olefins declines.

The effects of pressure on process selectivity can be interpreted by considering the olefins reactivity during low-temperature FTS. Increasing the pressure would generally result in the condensation

Table 4 – *Effect of pressure*

	Catalyst	*p* (bar)							
		1	3	5	7	9	11	13	15
CO conv. (%)	A	64.1	64.1	63.7	61.2	61.2	60.3	60.0	60.0
	B	58.6	56.7	54.0	53.1	53	52.4	52.1	51.3
Methane sel. (%)	A	20.7	20.2	19.7	18.4	17.3	16.4	15.4	12.8
	B	18.4	18.0	16.4	15.7	15.4	15.0	14.3	14.0
Olefin (C_2-C_4) sel. (%)	A	39.0	40.1	36.7	32.9	30.1	29.0	24.8	22.1
	B	37.2	32.4	29.3	28.6	26.2	25.2	22.6	21
C_{5+} sel. (%)	A	13.2	13.5	16.7	20.9	24.9	27.3	34.6	41.8
	B	13.9	16.8	25.9	26.8	28.9	30.0	36.6	40.8
CO_2 sel. (%)	A	6.0	4.6	4.4	4.3	4.3	4.2	4	4
	B	5.1	6	6.4	6.4	6.7	6.8	5.2	5

of hydrocarbons.[26] Under typical reaction conditions, a thin layer of liquid hydrocarbon covers the catalyst particles. As a result, before the reactants reach the catalyst surface they have to diffuse inside this layer, while reaction products have to do the same in the opposite direction before being desorbed. It is well known that olefins, in contrast to paraffins, can be readsorbed on the active sites, reinserted in the chain growth process, or can be hydrogenated to the corresponding paraffins.[27–29]

The results indicate that catalyst (B) has a higher C_{5+} selectivity and lower selectivity toward methane and light olefins than catalyst (A). In addition, at 3 bar, CO_2 selectivity is lower for catalyst (B) than (A).

Effect of space velocity

In Table 5, the CO conversion and the hydrocarbon formation and selectivity to CO_2 are given for different GHSVs varying from 1600 to 5600 h^{-1}. Since the amount of catalyst was kept constant during all experiments, the GHSV was changed by varying the syngas flow rate.

As expected, the conversion of CO declines with increased GHSV for both catalysts but this trend is marginal. It can be concluded that in this range of GHSVs the external mass transfer restriction is negligible. For catalyst (B) this reduction is more pronounced. For catalyst (A), selectivity to methane is reduced from 1600 to 2600 h^{-1}, and then

Table 5 – *Effect of GHSV on both CO conversion and selectivity*

	Catalyst	GHSV (h^{-1})				
		1600	2600	3600	4600	5600
CO conv. (%)	A	64.9	63.0	61.6	59.0	57.2
	B	57.2	54.1	50.4	47.2	45.3
Methane sel. (%)	A	22.4	20.7	21.4	21.9	23.1
	B	18.2	19.0	19.9	21.1	23.2
Olefin (C_2-C_4) sel. (%)	A	35.1	39.0	38.1	34.0	32.2
	B	29.2	30.5	32.1	34.5	29.1
C_{5+} sel. (%)	A	11.0	12.2	13.2	13.8	13.9
	B	7.0	8.1	9.1	9.9	10.5
CO_2 sel. (%)	A	6.0	6.4	6.8	7.1	7.2
	B	11.0	10.2	9.6	9.1	8.4

an increase is also observed. For catalyst (B), selectivity to methane increases systematically. The selectivity to light olefinic product is increased, while a declining trend is observed after GHSV = 3600 to 5600 h^{-1} for catalyst (A). For (B), space velocity did not have a significant effect on light olefinic product. Selectivity to C_{5+}, slightly increases upon increasing the space velocity for both catalysts. In general, the gas film diffusion effect plays a dominant role in the removal of hydrocarbons from the catalyst surface and external mass transfer limitations are eliminated with increasing GHSV. On the other hand, a high GHSV velocity (low residence time) decreases the temperature rise in the fixed-bed reactor, with the benefit of increasing heavy products selectivity.[30] The effects of space velocity (in the investigated range) on WGS activity are, however, very small for both catalysts.

After comparing performance of the two catalysts, it can be concluded that the incipient wetness catalyst (A) has a higher activity, higher light olefin selectivity, higher selectivity to C_{5+} and higher methane selectivity, as well as lower WGS activity.

Duration test

The incipient wetness catalyst (A) showed high activity in FTS reaction under the optimal conditions (H_2/CO = 2/1, p = 3 bar, GHSV = 2600 h^{-1} and ϑ = 260 °C). With respect to high selectivity to light olefin for co-precipitate catalyst (B) the highest activity was achieved at H_2/CO = 2/1, p = 1 bar at 240 °C and GHSV = 4600 h^{-1} as optimal operating conditions.

To study the catalyst under steady-state conditions, this catalyst was tested for a long run period. As shown in Figs 3 and 4, the CO conversion decreased by 15 % of the initial level and reached a stable level only after about 24 h on stream, and thereafter (24–240 h) the activity declined only about 3.0 %. Also, methane selectivity gradually

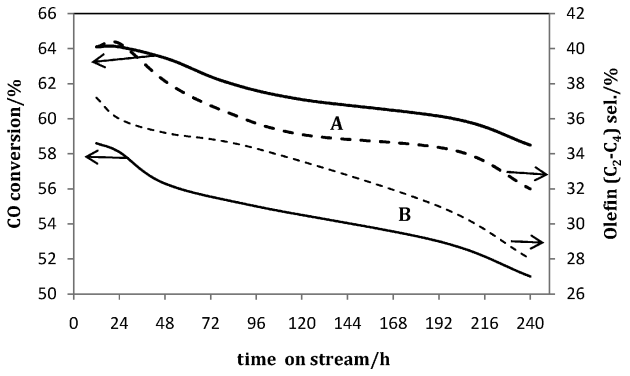

Fig. 3 – *CO conversion and selectivity to olefin for the duration of the test for catalysts A and B (under optimum experimental conditions for each catalyst)*

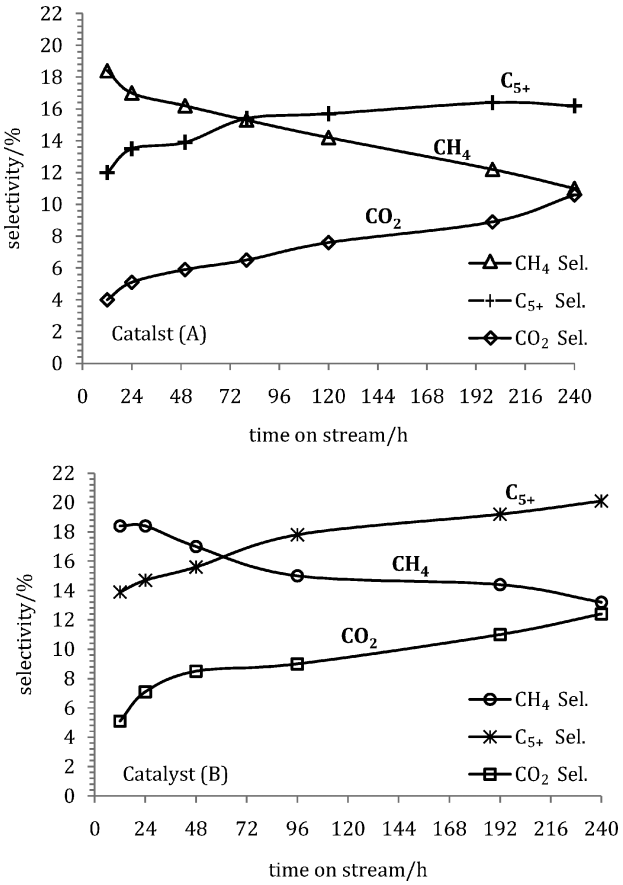

Fig. 4 – *Selectivity to methane, C_{5+} and CO_2 for the duration of the test for catalysts A and B (under optimum experimental conditions for each catalyst)*

decreased about 7.4 % during the period from 24 to 240 h. In contrast, C_{5+} selectivity increased about 4.2 % during this time. The selectivity toward light olefins declined only 3.2 %. Finally, the WGS activity increased about 6.6 %.

For catalyst (B), it was found that after stabilization (up to 48 h) the activity of catalyst declined only by about 6.4 % and selectivity toward light olefins and C_{5+} remained constant around 97 % during the FTS reaction. The methane selectivity declined by 4.2 %.

Based on the stable conversion from SEM micrographs (Fig. 2), it was shown that the size of metal crystallites increases during FTS. With respect to selectivity of products, it can be concluded that the larger particles are more selective to higher molecular mass hydrocarbons, and smaller iron particles are selective to methane and light gaseous hydrocarbons. The deactivation rate of the smaller particles, which are selective for methane production, is higher than that of the larger particles.[31] Therefore, smaller particles deactivate initially, leading to increase of C_{5+} selectivity and suppression of methane production. This could explain the rise in C_{5+} selectivity and the decline in methane se-

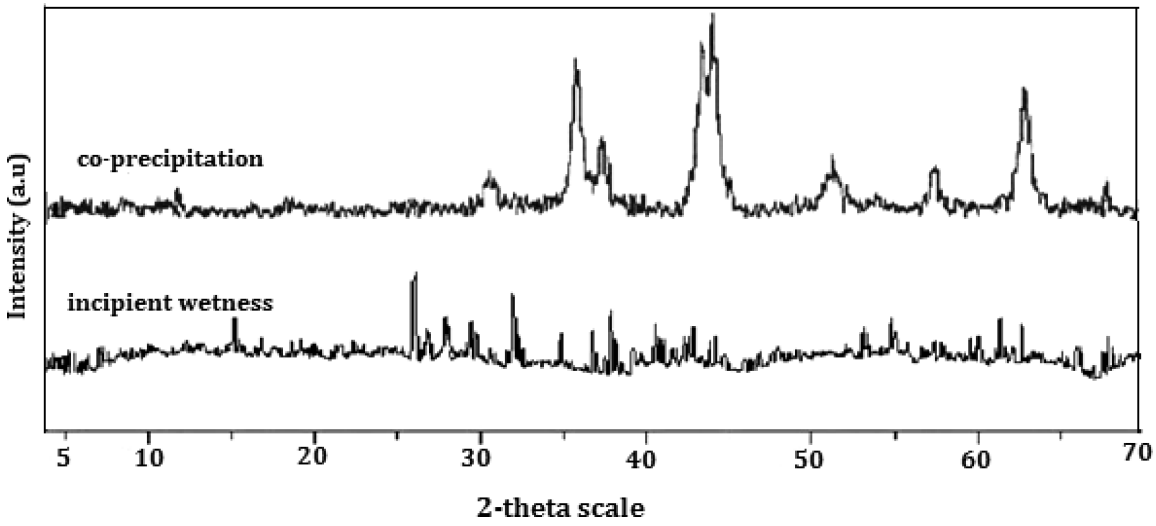

Fig. 5 – *XRD patterns for the used catalysts; bottom: catalyst (A) and top: catalyst (B)*

lectivity during the 240 h of FTS. Therefore, it can be concluded that the deactivation rate of the iron nickel catalyst is structure-dependent and is related to the size and nature of the iron particles that changed during the FTS reaction. Finally, as a result the higher iron dispersion enhances the negative effects of water such as low CO conversion, low olefin selectivity and higher methane and CO_2 selectivity especially at higher water partial pressures under FTS conditions.

As depicted in Fig. 5, the both used catalysts (after the FT reaction) have carbide (FeC, FeC_2, Fe_2C) and iron oxide (Fe_2O_3, Fe_3O_4) phases, both of which are active phases in the FTS catalysts. Reportedly, carbide phases are active in the hydrogenation of CO, and oxide phases have high selectivity for the production of olefins, and magnetite (Fe_3O_4) is the most active phase for water gas shift reaction.[16,21–24]

Conclusion

In this study, two methods were employed to the preparation of 40 % Fe/60 % Ni/40 % Al_2O_3 catalyst, namely the incipient wetness (catalyst A) and co-precipitate (catalyst B) procedure and the effect of inlet H_2/CO ratios, temperature, pressure and GHSV on the activity and hydrocarbon selectivity to especially light olefinic product has been studied. The optimum conditions were found to be 260 °C, H_2/CO = 2/1, GHSV = 2600 h^{-1} and 3 bar for (A), whereas 240 °C, H_2/CO = 2/1 GHSV = 4600 h^{-1} and 1 bar were the optimum operating conditions for catalyst (B). The results showed that these two catalysts were highly stable and retained their activity and selectivity for 240 h. However, catalyst (A) (incipient wetness catalyst) had higher activity, selectivity to light olefins and lower selectivity to methane and WGS activity at stable period. Therefore, it can be concluded that the deactivation rate of the iron nickel catalyst depends on structure and is related to the size and nature of the iron particles that changed during the FTS reaction.

ACKNOWLEDGMENT

The authors gratefully acknowledge University of Sistan and Baluchestan and National Iranian Oil Company (N.I.O.C) for helping and supporting this research.

Nomenclature

$N_{CO,in}$ – CO molar flow rates in the reactor feed, mol min^{-1}
$N_{CO,out}$ – CO molar flow rates in exit stream, mol min^{-1}
n_i – number of atom carbon for product ith
N_i – number of moles for product ith
$N_{C,out}$ – moles of carbon output
$N_{C,in}$ – moles of carbon input
θ – temperature, °C
p – pressure, bar
WGS – Water Gas Shift
GHSV – Gas Hourly Space Velocity

References

1. *Ahon, V. R., Lage, P. L. C., de Souza, C. D. D., Mendes, F. M., Schmal, M.,* Journal of Natural Gas Chemistry **15** (2006) 307.
2. *Dasgupta, D., Wiltowski, T.,* Fuel **90** (2011) 174.
3. *Dry, M. E.*, Catalysis Today **71** (2002) 227.
4. *De la Pena O'Shea, V. A., Alvarez-Galvan, M. C., Campos-Martin, J. M., Fierro, J. L. G.*, Applied Catalysis A **326** (2007) 65.

5. *Jager, B.*, Studies in Surface Science and Catalysis **119** (1998) 25.
6. *Tihay, F., Roger, A. C., Kiennemann, A., Pourroy, G.,* Catalysis Today **58** (2000) 263.
7. *Cooper, M. E., Forest, J.*, Applied Catalysis A **5** (1990) L5–L8.
8. *Feyzi, M., Irandoust, M., Mirzaei, A. A.*, Fuel Processing Technology **92** (2011) 1136.
9. *Mirzaei, A. A., Beig babaei, A., Galavy, M., Youssefi, A.*, Fuel Processing Technology **91** (2010) 335.
10. *Mirzaei, A. A., Faizi, M., Habibpour, R.*, Applied Catalysis A **306** (2006) 98.
11. *Atashi, H., Siami, F., Mirzaei, A. A., Sarkari, M.*, Journal of Industrial and Engineering Chemistry **16** (2010) 952.
12. *Park, C., Baker, R. T. K.*, Journal of Catalysis **190** (2000) 104.
13. *Vannice, M. A.*, Journal of Catalysis **44** (1976) 152.
14. *Ekerdt, J. G, Bell, A. T.*, Journal of Catalysis **62** (1980) 19.
15. *Baker, J. A., Bell, A. T.*, Journal of Catalysis **78** (1982) 165.
16. *Botes, F. G.*, Applied Catalysis A **328** (2007) 237.
17. *Pansanga, K, Lohitharn, N, Chien, A. C. Y., Lotero, E., Panpranot, J., Praserthdam, P., Goodwin, Jr, J., G.*, Applied Catalysis A **332** (2007) 130.
18. *Unmuth, E. E., Schwartz, L. H., Butt.*, Journal of Catalysis **63** (1980) 404.
19. *Mirzaei, A. A., Habibpour, R., Faizi, M., Kashi, E.,* Applied Catalysis A **301** (2006) 272.
20. *Ø Borg, S., Storsæter, Eri, S., Wigum, H., Rytter, E., Holmen, A.*, Catal. Lett **107** (2006) 95.
21. *Van der Laan, G. P., Beenackers, A. A. C. M.*, Applied Catalysis A **193** (2000) 39.
22. *Yang, J., Liu, Y., Chang, J., Wang, Y. N., Bai, L., Xu, Y. Y., Xiang, H. W., Li, Y. W., Zhong, B.*, Industrial and Engineering Chemistry Research **42** (2003) 5066.
23. *Tenga, B. T., Changa, J., Yang, J., Wang, G., Zhang, C. H., Xu, Y. Y., Xiang, H. W., Li, Y. W.*, Fuel **84** (2005) 917.
24. *Guo, X. H., Liu, Y., Chang, J., Bai, L., Xu, Y. Y., Xiang, H. W., Li, Y. W.*, Journal of Natural Gas Chemistry **15** (2006) 105.
25. *Tian, L., Huo, C. F., Cao, D. B., Yang, Y., Xu, J., Wu, B. S., Xiang, H. W., Xu, Y. Y., Li, Y. W.*, Journal of Molecular Structure: THEOCHEM **941** (2010) 30.
26. *Griboval-Constant, A., Khodakov, A. Y., Bechara, R., Zholobenko, V. L.*, Studies in Surface Science and Catalysis **144** (2002) 609.
27. *Bechara, R., Balloy, D., Vanhove, D.*, Applied Catalysis A **207** (2001) 34.
28. *Kuipers, E. W., Scheper, C., Wilson, J. H., Vinkenburg, I. H., Oosterbeek, H.*, Journal of Catalysis **158** (1996) 288.
29. *Van der Laan, G. P., Beenackers, A. A. C. M.*, Catalysis Reviews Science and Engineering **1** (1999) 255.
30. *Dry, M. E.,* In Catalysis Science and Technology; *Anderson, J. R., Boudert, M.,* Eds., Springer-Verlag: New York , 1981.
31. *Sari, A., Zamani, Y., Taheri, S. A.*, Fuel Processing Technology **90** (2009) 1305.